Cavitation onset caused by acceleration

Zhao Pan[a,1], Akihito Kiyama[b,1], Yoshiyuki Tagawa[b,2], David J. Daily[c,1], Scott L. Thomson[d], Randy Hurd[a], and Tadd T. Truscott[a,2]

[a]Department of Mechanical and Aerospace Engineering, Utah State University, Logan, UT 84322; [b]Department of Mechanical Systems Engineering, Tokyo University of Agriculture and Technology, Koganei, 184-8588 Tokyo, Japan; [c]Naval Undersea Warfare Center, Newport, RI 02841; and [d]Department of Mechanical Engineering, Brigham Young University, Provo, UT 84602

Edited by Jacob N. Israelachvili, University of California, Santa Barbara, CA, and approved June 22, 2017 (received for review February 14, 2017)

Striking the top of a liquid-filled bottle can shatter the bottom. An intuitive interpretation of this event might label an impulsive force as the culprit in this fracturing phenomenon. However, high-speed photography reveals the formation and collapse of tiny bubbles near the bottom before fracture. This observation indicates that the damaging phenomenon of cavitation is at fault. Cavitation is well known for causing damage in various applications including pipes and ship propellers, making accurate prediction of cavitation onset vital in several industries. However, the conventional cavitation number as a function of velocity incorrectly predicts the cavitation onset caused by acceleration. This unexplained discrepancy leads to the derivation of an alternative dimensionless term from the equation of motion, predicting cavitation as a function of acceleration and fluid depth rather than velocity. Two independent research groups in different countries have tested this theory; separate series of experiments confirm that an alternative cavitation number, presented in this paper, defines the universal criteria for the onset of acceleration-induced cavitation.

cavitation | accelerating fluid | bubble formation | vaporization | bubble collapse

Cavitation can occur in a liquid instantly set into motion by an impulsive force. The collapse of the cavitation bubbles often results in severe damage to the container. Examples include a popular trick where striking the top of an opened long-neck bottle can cause the bottom to shatter due to cavitation near the base of the bottle (Fig. 1*A* and ref. 1). Similarly, dropping a liquid-filled glass tube on the floor can introduce cavitation, leading to crack formation on the tube wall (Fig. 1*B* and refs. 2 and 3). More commonly, sudden valve closing inside of a water pipe can cause a loud hammering sound due to the collapse of cavitation, resulting in damage on the inner walls (4). The effects of blast and impact that cause traumatic brain injury from cavitation have also been investigated (5, 6). To avoid cavitation-induced damage (7–9), it is crucial to predict the onset of cavitation.

Cavitation onset in a high-speed flow [e.g., flow around propellers and in pumps (10)] can be characterized using a variant of the Euler number known as the cavitation number (11, 12). The cavitation number is typically of the form

$$C = \frac{p_r - p_v}{\frac{1}{2}\rho v^2}, \qquad [1]$$

where p_r is the reference pressure, p_v is the liquid vapor pressure, ρ is the liquid density, and v is the local velocity (13–16). This cavitation number is a ratio of the pressure difference to the pressure drop due to the fluid momentum. The large momentum of the fluid dominates when $C \ll 1$, inducing cavitation. However, when $C \gg 1$, the pressure at all locations is above the threshold for bubble formation, making cavitation unlikely. Practically, several advanced coefficients have been proposed to estimate cavitation inception for various geometries (16).

However, the conventional cavitation number (C) could incorrectly predict the cavitation onset in a liquid accelerated in a short amount of time. For example, the cavitation event that breaks the bottle in Fig. 1*A* has a maximum velocity of $v \approx 2$ m/s, which yields the cavitation number $C \sim O(10^2)$. For the falling tube case in Fig. 1*B* a similar calculation leads to $C \sim O(10^2)$ (Table S1), whereas the conventional cavitation number requires $C \ll 1$ (16). Thus, a new cavitation number is required to define the physics of cavitation onset.

In the past, researchers have conducted similar experiments with a bullet-piston device to predict the tensile strength of a liquid, including pure water (17). They reported that the cavitation may occur in the liquid due to dynamic stresses imposed by acceleration, but not the conditions for cavitation onset (18, 19). Recently, the authors have proposed an alternate cavitation number (1, 20) based on the earlier formulation of ref. 11 and found partial validation by conducting a few experiments. However, existing experimental reports (3, 21, 22) have limited parameter space or are supported solely by numerical simulations (23), which was unsatisfactory for a full validation of an alternative cavitation number.

To predict and summarize cavitation onset by large accelerations we present a derivation of an alternative cavitation number based on the equation of motion (11), which modifies the fluid inertial term (denominator of Eq. **1**) to include acceleration. We find good agreement with experimental results from our two independent research groups. Although the experimental setup of each group is different, the data support the same theory.

Theory

We propose an alternative cavitation number based on acceleration. Consider a vertical, cylindrical column of liquid undergoing an impulsive acceleration in the vertical direction as shown in Fig. 2. Based on the assumption that the liquid is inviscid and incompressible and has a velocity magnitude significantly smaller than the acceleration ($\partial v/\partial t$), as is commonly known (11, 24–26), only the pressure gradient and acceleration remain (11), and the Navier–Stokes equations are reduced to

Significance

In this paper we propose an alternative derivation of the cavitation number and validate the threshold. The proposed dimensionless number is more suitable to predict the cavitation onset caused by a sudden acceleration rather than a large velocity as prescribed by the traditional cavitation number. Systematic experiments were conducted for validation, confirming that the alternative cavitation number predicts the threshold at which cavitation will occur ($Ca < 1$).

Author contributions: Y.T. and T.T.T. designed research; Z.P., D.J.D., and T.T.T. contributed new analytic tools; Z.P., A.K., and D.J.D. analyzed data; and Z.P., A.K., Y.T., D.J.D., S.L.T., R.H., and T.T.T. wrote the paper.

The authors declare no conflict of interest.

This article is a PNAS Direct Submission.

Freely available online through the PNAS open access option.

[1]Z.P., A.K., and D.J.D. contributed equally to this work.

[2]To whom correspondence may be addressed. Email: tagawayo@cc.tuat.ac.jp or taddtruscott@gmail.com.

This article contains supporting information online at www.pnas.org/lookup/suppl/doi:10.1073/pnas.1702502114/-/DCSupplemental.

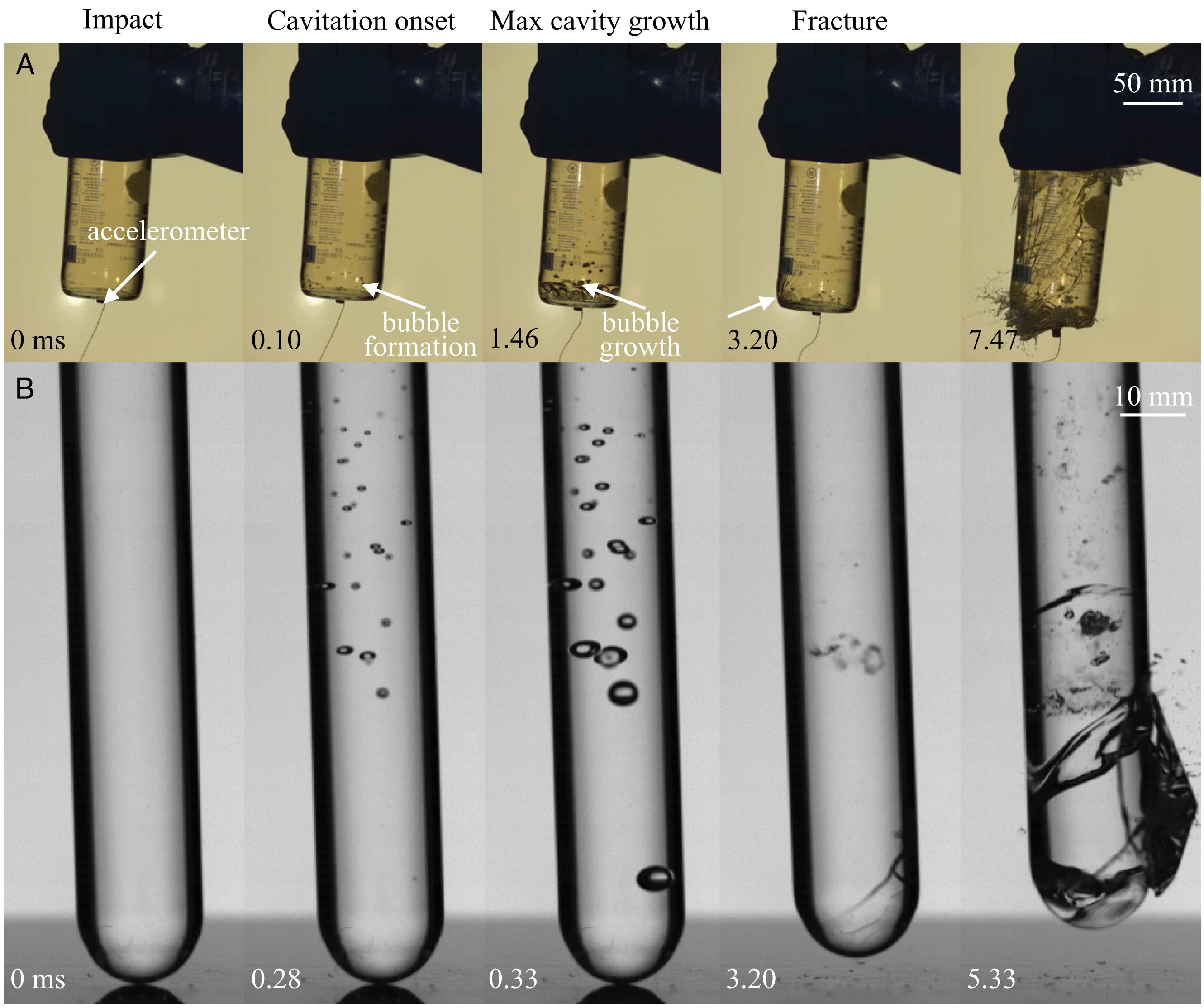

Fig. 1. Two cases of cavitation onset introduced by large accelerations in low-speed flows. A bottle filled with water accelerated by the impact of a mallet on the top (*A*). A test tube filled with silicone oil accelerated by an impact with the ground (*B*). Both image sets correspond to the impact (first frame), tiny bubble appearance (second frame), bubble expansion (third frame), bubble collapse and cracking (fourth frame), and crack propagation/failure (fifth frame). Although the time between each event is different, the overall behavior is very similar (Movies S1–S4). Relative timing of bubble collapse and fracture incidence suggests that implosion-induced waves are likely responsible for fracture initiation, although further investigation into fracture mechanisms in the case studies presented here would be necessary to confirm this observation (Fig. S1). Relationships between cavitation and structural damage are well-documented elsewhere in biological and man-made systems (27–31).

$$\frac{\partial v}{\partial t} = -\frac{1}{\rho}\nabla p. \quad [2]$$

Integrating Eq. **2** along the centerline of the liquid from the free surface to the bottom of the column (assuming the depth of the liquid is h), denoting the magnitude of the vertical component of $\partial v/\partial t$ as a, and solving for the pressure difference in the liquid column yields

$$p_r - p_b = \rho a h, \quad [3]$$

where p_r is the reference pressure at the free surface and p_b is the pressure at the bottom of the column. Cavitation is likely to occur when $p_b < p_v$. Thus, we can establish

$$Ca = \frac{p_r - p_v}{\rho a h} \quad [4]$$

as an indicator of cavitation onset when the flow undergoes a violent acceleration. We refer to this expression as the quiescent cavitation number.

To gain physical insight into the interpretation of the quiescent cavitation number, gravitational acceleration can be introduced and Eq. **4** can be reformulated as

$$Ca = \frac{(p_r - p_v)/\rho g h}{a/g}. \quad [5]$$

Gravitational acceleration is not an essential term in the cavitation number. However, it is included here to enable a formulation with explicit physical meaning. The numerator is the maximum nondimensionalized force that the pressure difference can provide (similar to Eq. **1**) and the denominator is the nondimensionalized inertial force the liquid experiences under acceleration (in contrast to the fluid momentum of Eq. **1**). Thus, once the inertial forces exceed the maximum pressure difference (i.e., $Ca < 1$), cavitation is likely. However, when $Ca > 1$ the pressure is large enough to balance the vacuum introduced by acceleration. Hence, cavitation is not likely.

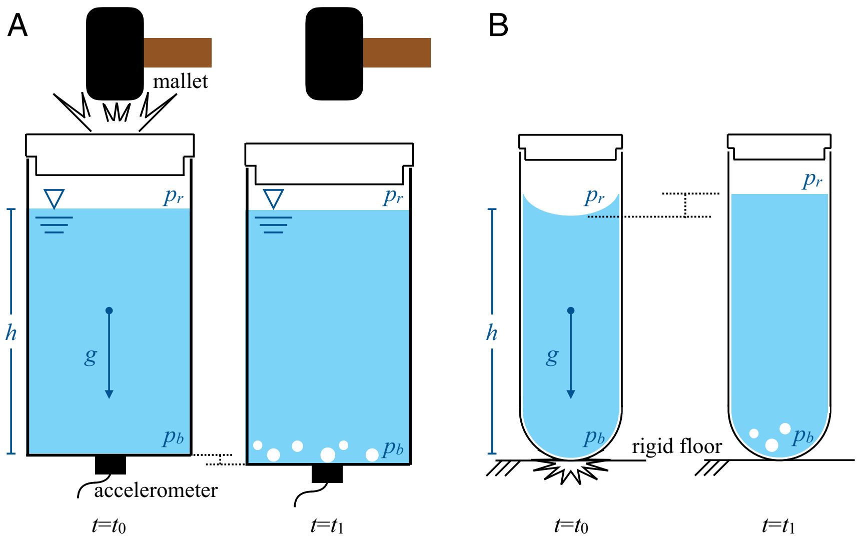

Fig. 2. Free body diagram of the fluid column: mean liquid column height (h), reference pressure (p_r), pressure at the bottom of the container (p_b), and gravitational acceleration (g). Experiment done at USU/BYU facilities (*A*), where the impact is imparted by a rubber mallet. The TUAT experiment uses a glass test tube with a rounded bottom, where the impact is imparted by collision with the ground (*B*). The small difference traveled between t_0 and t_1 is shown as dashed lines to emphasize the relative acceleration (experimental evidence shown in Fig. S2 and Movie S4).

Experimental Setup

More details about the experiments can be found in *Materials and Methods*. Two separate groups independently conducted the following experiments with different setups and measurement techniques to validate Eq. **4** or **5**.

The group from Utah State University and Brigham Young University (USU/BYU) used a cylindrical cavitation tube built from transparent acrylic (1, 20). The cavitation tube was fitted with a pressure tap to control internal pressure and an accelerometer with a maximum measurable acceleration of 1,000 g

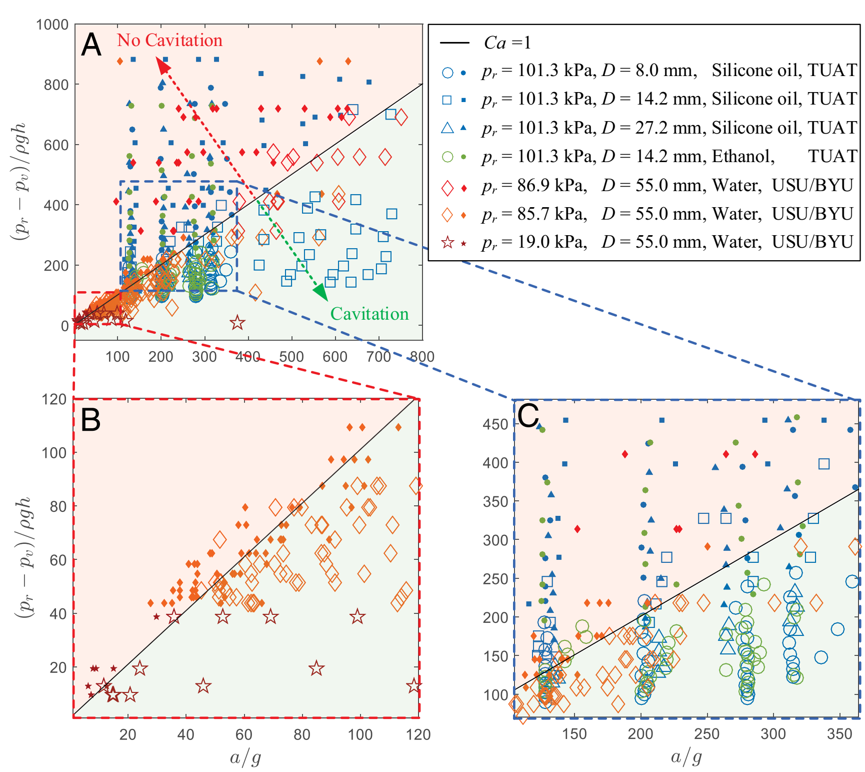

Fig. 3. Phase diagram for the cavitation onset by acceleration in the $\{(p_r - p_v)/\rho gh,\ a/g\}$ plane (*A*) for various fluid types, container diameters (D), pressures (p_r), and fluid depths (h) as marked in the legend. Open markers denote cavitation detection and filled markers denote absence of cavitation detection. Lines represent theoretical separation between cavity formation (shaded in red) and none (shaded in green) based on $Ca = 1$ in Eq. **5**. Changing the stiffness of the container and a nonfluid medium was also investigated as shown in Figs. S3 and S4 and Table S2. Close-up view (*B*) of concentrated data points in the region where the reference pressure was varied (red-squared region in *A*). Close-up view (*C*) of collapsed data points in the region where the fluid type was varied (blue-squared region in *A*).

(Figs. 2*A* and 1*A*). The experiment was performed with internal reference pressures (p_r) of 85.7, and 19.0 kPa. A high-speed camera was used to image the cavitation tube to detect the presence of cavitation bubbles. The cavitation tube was filled with distilled water to various depths (h) and the tube was accelerated by striking the top with a rubber mallet.

The group from Tokyo University of Agriculture and Technology (TUAT) used glass test tubes filled with silicone oil or ethanol of varying depth (h) impacting vertically on a flat rigid surface after free fall (Figs. 1*B* and 2*B*). The acceleration and appearance of cavitation bubbles was estimated with calibrated high-speed video.

Results and Discussion

Fig. 3 reports the experimental results from the two groups; oranges and reds are from the USU/BYU group and blues and greens are from the TUAT group. The vertical axis and the horizontal axis show the numerator and the denominator of Eq. **5**, respectively. Open markers represent cavitation detection and closed markers represent no cavitation. The black solid line is plotted according to $Ca = 1$. Most of the open markers are distributed in the region of $Ca < 1$ (shaded green in Fig. 3). However, closed markers dominate the region where $Ca > 1$ (shaded orange in Fig. 3). These results indicate that the proposed cavitation number explains the trend for a wide range of accelerations and water column depths.

The influence of the reference pressure p_r is shown in Fig. 3*B* and the influence of diameter and fluid type in Fig. 3*C* as zoomed-in regions of Fig. 3*A*. In contrast to the more difficult to apply or ambiguous result of the conventional cavitation number $C \ll 1$ and the values proposed by numerical simulation $Ca \ll 1$ (23), our data suggest that the onset of cavitation is located in a region near $Ca < 1$, regardless of the reference pressure, inner diameter of the tube, liquid column height, and fluid type.

Summary

In this paper we introduced an alternative formulation of the cavitation number that captures the cavitation onset caused by acceleration. In practice, the conventional cavitation number C (Eq. **1**) can inaccurately predict that no cavitation will occur when cavitation may, in fact, be occurring in suddenly accelerated flows. For example, the impact of a fluid-filled bottle with the ground can cause cavitation (Fig. 1) although the velocities are too small to predict using C. Thus, we propose an alternative cavitation number Ca (Eq. **4**) by applying the equation of motion, resulting in a replacement of the momentum term in C (velocity) with an inertial one in Ca (acceleration) in cases of acceleration-induced cavitation. Multiple sets of independent experiments were conducted by two separate groups to test the theory. Results show that cavitation occurs for $Ca < 1$ (Eq. **3**), consistent with the theoretical prediction, establishing that the alternative cavitation number Ca is a reasonable criterion for the onset of acceleration-induced cavitation. The alternative cavitation number can potentially be used as a criterion for brain injury caused by impact-induced cavitation (5, 6), prediction of water hammer (4), and potentially applied to the development of safety devices (e.g., helmet design).

Materials and Methods

USU/BYU Experiments. An acrylic tube (55.0 mm inner diameter) is partially filled ($h = 1-200$ mm) with distilled water ($\rho = 1.0 \times 10^3$ kg/m^3, $p_v = 2.3 \times 10^3$ Pa, and $\nu = 1$ cSt). Acceleration is introduced by striking the top of the tube with a mallet. The pressure in the tube is controlled by a vacuum. An accelerometer is connected to the bottom of the tube. The tube is illuminated by a backlight and images are recorded by a high-speed camera [Photron APX, SA-3, or Phantom V-1610, 3,000 to 100,000 frames per s (fps) and 0.1 mm per pixel]. Note that a very short paper focusing primarily on the artistic nature of a similar set of photographs rather than the scientific findings was recently published (1) and an early derivation of *Ca* was given in ref. 20.

TUAT Experiments. A glass test tube (inner diameter 8.0–27.2 mm, tube thickness $\approx$1 mm) is partially filled ($h = 5-120$ mm) with silicone oil ($\rho = 1.0 \times 10^3$ kg/m^3, $p_v = 7.0 \times 10^2$ Pa, and $\nu = 10$ cSt) or ethanol ($\rho = 8.0 \times 10^2$ kg/m^3 and $p_v = 6.0 \times 10^3$ Pa, and $\nu = 1$ cSt). The tube is held above the floor (22–135 mm) by an electromagnet until it is released. The tube is illuminated by a backlight and images are recorded by a high-speed camera (Photron SA-X, up to 90,000 fps and 0.1 mm per pixel). The basic concept of the experimental setup is similar to previous research (3, 24). Acceleration, *a*, is determined by the high-speed camera images, measuring the impact speed (sum of the downward speed of the tube just before the impact and the upward speed just after the impact) and dividing the impact speed by the duration of the collision of the tube bottom with the floor (32). Note that results appearing in this paper mirror our previous report (3) that focused on the motion of the gas–liquid interface rather than the onset of cavitation.

ACKNOWLEDGMENTS. A.K. and Y.T. thank Y. Noguchi, C. Kurihara, K. Hirose, Y. Watanabe, M. Maeshima, Y. Mukai, H. Kudo, K. Hayasaka, and R. Yukisada for their help during experiments. This work was supported by Japan Society for the Promotion of Science KAKENHI Grants 26709007, 16J08521, and 17H01246. This paper was partially written while A.K. was visiting the Department of Mechanical and Aerospace Engineering, Utah State University. A.K. acknowledges financial support from Tokyo University of Agriculture and Technology. T.T.T. pursued the study first at Brigham Young University and finalized these ideas and helped write the paper while at Utah State University.

1. Daily J, et al. (2014) Catastrophic cracking courtesy of quiescent cavitation. *Phys Fluid* 26:091107.
2. Milgram JH (1969) The motion of a fluid in a cylindrical container with a free surface following vertical impact. *J Fluid Mech* 37:435–448.
3. Kiyama A, Tagawa Y, Ando K, Kameda M (2016) Effects of a water hammer and cavitation on jet formation in a test tube. *J Fluid Mech* 787:224–236.
4. Bergant A, Simpson AR, Tinseling AS (2006) Water hammer with column separation: A historical review. *J Fluids Struct* 22:135–171.
5. Rosenfeld JV, et al. (2013) Blast-related traumatic brain injury. *Lancet Neurol* 12:882–893.
6. Hong Y, Sarntinoranont M, Subhash G, Canchi S, King MA (2016) Localized tissue surrogate deformation due to controlled single bubble cavitation. *Exp Mech* 56:97–109.
7. Benjamin TB, Ellis AT (1966) The collapse of cavitation bubbles and the pressures thereby produced against solid boundaries. *Philos Trans R Soc Lond A Math Phys Eng Sci* 260:221–240.
8. Brujan EA, Nahen K, Schmidt P, Vogel A (2000) Dynamics of laser-induced cavitation bubbles near elastic boundaries: Influence of the elastic modulus. *J Fluid Mech* 433:283–314.
9. Popinet S, Zaleski S (2002) Bubble collapse near a solid boundary: A numerical study of the influence of viscosity. *J Fluid Mech* 464:137–163.
10. Brennen C (1994) *Hydrodynamics of Pumps* (Oxford Univ Press, Oxford).
11. Batchelor G (1967) *An Introduction to Fluid Mechanics* (Cambridge Univ Press, Cambridge, UK).
12. Brennen C (1995) *Cavitation and Bubble Dynamics* (Oxford Univ Press, Oxford).
13. Barneblatt G (1987) *Dimensional Analysis* (Gordon and Breach, New York).
14. Gukhman A (1965) *Introduction to the Theory of Similarity* (Academic, New York).
15. White F (2005) *Viscous Fluid Flow* (McGraw-Hill, New York), 3rd Ed.
16. Arndt REA (1981) Cavitation in fluid machinery and hydraulic structures. *Annu Rev Fluid Mech* 13:273–326.
17. Williams PR, Williams RL (2004) Cavitation and the tensile strength of liquids under dynamic stressing. *Mol Phys* 102:2091–2102.
18. Morch KA (1982) Energy considerations on the collapse of cavity clusters. *Appl Sci Res* 38:313–321.
19. Williams PR, Williams RL (2002) Cavitation of liquids under dynamics stressing by pulses of tension. *J Phys D Appl Phys* 35:2222–2230.
20. Daily DJ (2013) Fluid-structure interactions with flexible and rigid bodies. PhD thesis (Brigham Young University, Provo, UT).
21. Kiyama A, Noguchi Y, Tagawa Y (2014) [The generation of a liquid jet induced by a pressure impulse (experimental study on the jet velocity)]. *Trans* JSME 80:FE0151. Japanese.
22. Chen QD, Wang L (2004) Production of large size single transient cavitation bubbles with tube arrest method. *Chin Phys* 13:564–570.
23. Fatjo GGA (2016) New dimensionless number to predict cavitation in accelerated fluid. *Int J Comput Methods Exp Measurements* 4:484–492.

24. Antkowiak A, Bremond N, Dizes SL, Villermaux E (2007) Short-term dynamics of a density interface following an impact. *J Fluid Mech* 577:241–250.
25. Krechetnikov R (2014) Flow around a corner in the water impact problem. *Phys Fluid* 26:072107.
26. Cooker MJ, Peregrine DH (1995) Pressure-impulse theory for liquid impact problems. *J Fluid Mech* 297:193–214.
27. Knapp RT (1955) Recent investigations of the mechanics of cavitation and cavitation damage. *Trans ASME* 77:1045–1054.
28. Plesset M, Ellis A (1955) On the mechanism of cavitation damage. *Trans ASME* 77:1055–1064.
29. Versluis M, Schmitz B, von der Heydt A, Lohse D (2000) How snapping shrimp snap: Through cavitating bubbles. *Science* 289:2114–2117.
30. Chen YL, Israelachvili J (1991) New mechanism of cavitation damage. *Science* 252:1157–1160.
31. Chen YL, Kuhl T, Israelachvili J (1992) Mechanism of cavitation damage in thin liquid films: Collapse damage vs. inception damage. *Wear* 153:31–51.
32. Young FR (1989) *Cavitation* (McGraw-Hill, New York).